JACS
JOURNAL OF THE AMERICAN CHEMICAL SOCIETY
Communication
pubs.acs.org/JACS

Mono-cadmium vs Mono-mercury Doping of Au_{25} Nanoclusters

Chuanhao Yao,[†,§] Yue-jian Lin,[‡,§] Jinyun Yuan,[∥,§] Lingwen Liao,[†] Min Zhu,[†] Lin-hong Weng,*[,‡] Jinlong Yang,*[,∥] and Zhikun Wu*[,†]

[†]Key Laboratory of Materials Physics, Anhui Key Laboratory of Nanomaterials and Nanostructures, Institute of Solid State Physics, Chinese Academy of Sciences, Hefei, Anhui 230031, China

[‡]Shanghai Key Laboratory of Molecular Catalysis and Innovative Material, Department of Chemistry, Fudan University, Shanghai 200433, China

[∥]Hefei National Laboratory for Physics Sciences at the Microscale, University of Science and Technology of China, Hefei, Anhui 230026, China

Supporting Information

ABSTRACT: Controlling the dopant type, number, and position in doped metal nanoclusters (nanoparticles) is crucial but challenging. In the work described herein, we successfully achieved the mono-cadmium doping of Au_{25} nanoclusters, and revealed using X-ray crystallography in combination with theoretical calculations that one of the inner-shell gold atoms of Au_{25} was replaced by a Cd atom. The doping mode is distinctly different from that of mono-mercury doping, where one of the outer-shell Au atoms was replaced by a Hg atom. $Au_{24}Cd$ is readily transformed to $Au_{24}Hg$, while the reverse (transformation from $Au_{24}Hg$ to $Au_{24}Cd$) is forbidden under the investigated conditions.

Compared with bulk metal materials, metal nanoparticles have received ever increasing interest over the past decades.[1−3] In particular, doped metal nanoparticles are currently a focus of attention due to their intriguing properties and promising applications.[4−11] However, their structures unraveling at the atomic level hinder some insightful structure−property correlations. Fortunately, the ultrasmall (<2 nm) thiolated metal nanoclusters (including their alloy counterparts) developed recently provide opportunities to gain such insights.[12−32] Of note, being more or less molecular species, thiolated metal nanoclusters differ from the so-called metal nanoparticles (dimensions ranging between 2 and 100 nm) not only in size but also in structure and properties.[15−19] They are also different from organometallic clusters (including bimetal[33,34] or even trimetal[35,36] clusters) in the featured metal core,[15−19] the absence of a metal−carbon bond,[15−19] etc. Herein, we focus on well-defined doped thiolated nanoclusters (DTNs),[22−27] which provide ideal models for studying the structure−property correlation. After the report of $Au_{24}Pd$ by Murray's group[37] and by Negishi's group,[38] a number of DTNs, including $Au_{24}Pt$,[25,26] $Au_{25-x}Ag_x$,[39,40] $Au_{144-x}Ag_x$,[41] $Au_{38-x}Ag_x$,[42] $Au_{144-x}Cu_x$,[43] and $Ag_{24}Pt(Pd)$,[44] were successively synthesized by reducing mixed metal thiolates (synchro-synthesis). However, no DTNs with atomic mono-dispersity except for $Au_{24}Pd(Pt)$[25,26,37,38] and $Ag_{24}Pt(Pd)$[44] have been obtained by synchro-synthesis until now. Galvanic reduction (GR)[45−54] is another popular way to synthesize nano-bimetals, but atomically mono-disperse DTNs have not been obtained so far by this method, possibly due to its uncontrollable spontaneity. Overall, obtaining atomically mono-disperse DTNs, which is crucial to understand the effects of doping, is still challenging. Fortunately, our recent finding (anti-galvanic reduction, AGR)[55−57] provides a novel strategy for the synthesis of DTNs that are otherwise difficult to obtain, and very recently, the silver DTN $Au_{25}Ag_2(PET)_{18}$[56] and the mono-mercury DTN $Au_{24}Hg(PET)_{18}$[57] (where PET = SC_2H_4Ph) were synthesized using this unexpected method. It is interesting to compare the two doping modes. For $Au_{25}Ag_2(PET)_{18}$, the two Ag atoms deposit on the surface of $Au_{25}(PET)_{18}$ without Au being replaced by Ag, while for the latter, one Au atom in the outer shell of $Au_{25}(PET)_{18}$ is replaced by a Hg atom (see Figure S1). Intriguing questions naturally arise: Can this unique doping method be extended to active metals (those metals lying ahead of H in the galvanic series), and, if so, where do the active metal dopants go?

To unravel these questions, the most extensively studied nanocluster—$[Au_{25}(PET)_{18}]^-$ ($[Au_{25}]^-$ for short; counterion, $N(C_8H_{17})_4^+$)[16,17,58]—was chosen as the matrix, and the common divalent Zn^{2+}, Co^{2+}, Ni^{2+}, and Cd^{2+} were chosen as active metal ions, respectively. In a typical AGR reaction, $[Au_{25}]^-$ (Figure S2) was first dissolved in acetonitrile, after which a freshly prepared acetonitrile solution of $Cd(NO_3)_2$, $Co(NO_3)_2$, $Ni(NO_3)_2$, or $Zn(NO_3)_2$ was added. The reaction was carried out at 60 °C in a water bath for 0.5 h (details are provided in the Supporting Information). The UV/vis/NIR absorption spectra of the crude products obtained from the four reactions clearly show some notable discrepancies (Figure S3). In the case of the reaction between $[Au_{25}]^-$ and Zn^{2+}, there are three absorption peaks for the product centered at 385, 470, and 658 nm, which are in good agreement with those of cationic $Au_{25}(PET)_{18}$ ($[Au_{25}]^+$ for short),[59−61] see Figure S3a. In the cases of Co^{2+} and Ni^{2+}, the UV/vis/NIR absorption spectra of the products are almost superimposable (Figure S3b,c), indicating that their products may be identical. By comparison with that of $[Au_{25}]^-$,[17,59] the ∼400 nm peak of the product becomes more prominent while the ∼450 nm peak becomes less distinct concurrently. The ∼680 nm peak slightly redshifts to ∼687 nm, and the ∼800 nm shoulder peak that is a fingerprint of the negatively charged $[Au_{25}]^-$ becomes ambiguous, indicating that $[Au_{25}]^-$ is oxidized

Received: September 13, 2015
Published: November 23, 2015

ACS Publications © 2015 American Chemical Society

DOI: 10.1021/jacs.5b09627
J. Am. Chem. Soc. 2015, 137, 15350−15353

to a neutral $Au_{25}(PET)_{18}$ ($[Au_{25}]^0$ for short)[62,63] in both cases. In Figure S3d, the relative intensity of the shoulder peak at 450 nm for $[Au_{25}]^-$ [17,58] further decreases and redshifts to ~470 nm, while the peak at ~680 nm slightly blueshifts to ~677 nm, which implies that $[Au_{25}]^-$ was probably transformed to some novel nanoparticles. Herein we give a short discussion to the absorption change of $[Au_{25}]^-$. Due to quantum confinement of electrons in the Au nanoclusters, they exhibit discrete electronic structure (e.g., HOMO−LUMO gap) and molecule-like optical properties.[17] Their electronic structure is susceptible, resulting in fingerprint absorption which is highly sensitive to composition (structure),[25,37,38] charge state,[17,61,63] etc. Thus, it is not difficult to figure out that $[Au_{25}]^-$ shows different UV/vis/NIR spectra depending on the salts due to their various oxidability or doping ability, which also somehow provides references for choosing suitable metal salts for the doping. It is worth noting that, at this point, it is very difficult to predict the reaction between $[Au_{25}]^-$ and some metal salts due to the complexity of such reactions.

Matrix-assisted laser desorption/ionization time-of-flight mass spectrometry (MALDI-TOF-MS) was employed to further analyze the products. As shown in Figure 1, a distinct mass

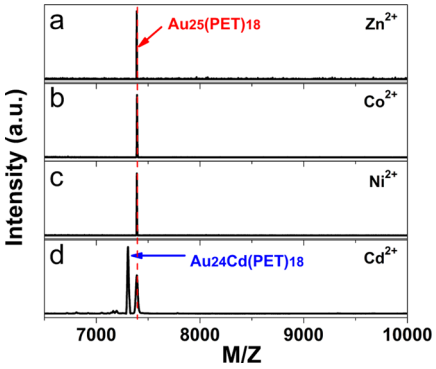

Figure 1. MALDI-TOF-MS of the products obtained from the reaction between $[Au_{25}]^-$ and Zn^{2+} (a), Co^{2+} (b), Ni^{2+} (c), or Cd^{2+} (d).

peak at $m/z \approx 7394$ is observed in all cases, which indicates that the Au_{25} ($[Au_{25}]^q$, $q = -1, 0, +1$) structure exists in all cases (but may bear different charge states). Taking their absorption spectra into consideration and making a careful comparison with the absorption of differently charged Au_{25} shown in Figure S4, one can conclude that $[Au_{25}]^-$ is oxidized to $[Au_{25}]^0$ by $Ni(NO_3)_2$ and $Co(NO_3)_2$ and to $[Au_{25}]^+$ by $Zn(NO_3)_2$. For the case of reaction between $[Au_{25}]^-$ and $Cd(NO_3)_2$, some new species is detected in the mass spectrum of the product: Besides the peak of Au_{25}, a dominant peak at $m/z \approx 7309$ is also observed in Figure 1d, and the ~85 (m/z) deviation from the Au_{25} peak implies that it may correspond to $Au_{24}Cd(PET)_{18}$; i.e., one Au atom in $Au_{25}(PET)_{18}$ is replaced by a Cd atom ($M_{Au} - M_{Cd} = 84.6$ Da). The excellent agreement between the experimental and calculated isotopic patterns of $Au_{24}Cd(PET)_{18}$ further confirms the assignment (see Figure 2). Thus, two clusters (major $Au_{24}Cd(PET)_{18}$ and minor $Au_{25}(PET)_{18}$) were produced from the reaction of $[Au_{25}]^-$ with $Cd(NO_3)_2$, deduced from the mass spectrum.

How to purify $Au_{24}Cd(PET)_{18}$ remains a challenge. Inspired by Jin's work, where $Au_{24}Pt(PET)_{18}$ was successfully isolated from the mixture of $Au_{24}Pt(PET)_{18}$ and $Au_{25}(PET)_{18}$ by the addition of H_2O_2,[25] we are fortunate to obtain pure $Au_{24}Cd(PET)_{18}$ with 56% yield (based on Au atom in the starting $[Au_{25}]^-$) by using an etching method. The reason is that

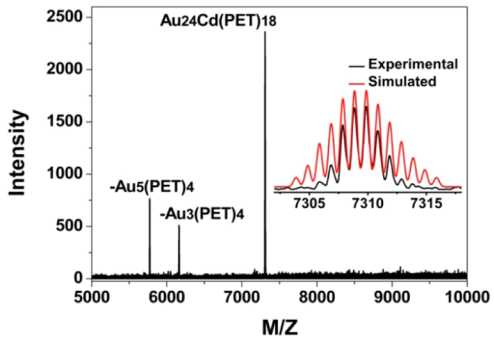

Figure 2. MALDI-TOF-MS spectrum of pure $Au_{24}Cd(PET)_{18}$.

$Au_{24}Cd(PET)_{18}$ is more stable than $Au_{25}(PET)_{18}$ and can endure the etching, while the less stable $Au_{25}(PET)_{18}$ decomposes after exposure to excess phenylethanethiol. The purity of $Au_{24}Cd(PET)_{18}$ is evidenced by the combination of MALDI-TOF-MS (Figure 2) and UV/vis/NIR (Figure S5), and further supported by thermogravimetric analysis (TGA): A weight loss of 33.5 wt% for the as-obtained $Au_{24}Cd(PET)_{18}$ is in good agreement with the theoretical value (33.8 wt%; Figure S6). By carefully comparing the absorption spectra of purified and unpurified $Au_{24}Cd(PET)_{18}$ (Figure S5), one can conclude that the enclosed $Au_{25}(PET)_{18}$ in the crude product of the reaction between $[Au_{25}]^-$ and Cd^{2+} is neutral. The dissolubility of the crude product in acetonitrile gives further support for the neutrality of the enclosed Au_{25} species, or else the negatively or positively charged Au_{25} will be dissolvable in CH_3CN.[13,16,17,59] Thus, the reaction of $[Au_{25}]^-$ with $Cd(NO_3)_2$ results in $Au_{24}Cd(PET)_{18}$ and $[Au_{25}]^0$. It is interesting that of the four investigated active metals, only Cd can be incorporated into Au_{25}, most likely because Cd and Au atoms have similar sizes and electronic structures (like is compatible with like, i.e., "birds of a feather flock together"), which is also supported by our previous doping of Hg to $[Au_{25}]^-$.[57] To get details about such replacement by Cd or Hg, it is interesting but very difficult to probe in situ. A possible process is proposed for that: First, Hg^{2+} or Cd^{2+} is reduced by reductive $[Au_{25}]^-$ (AGR), and then exchanges with a single Au atom in Au_{25}, resulting in the formation of $Au_{24}Cd(Hg)$ and Au^+ (which was indicated by mass spectrometry, see Figure S7). Owing to the limited reducibility of $[Au_{25}]^-$, it cannot reduce more than one Hg^{2+} or Cd^{2+}; thereby, only one Hg or Cd atom is doped to $[Au_{25}]^-$. The whole reaction can be represented by the following equation: $[Au_{25}]^- + Hg(Cd)^{2+} \rightarrow Au_{24}Hg(Cd) + Au^+$ (the counterions are omitted for clarity).

The structure of $Au_{24}Cd(PET)_{18}$, as revealed by single-crystal X-ray crystallography (at 123 or 258 K), remains a framework of $Au_{25}(PET)_{18}$ with one inner-shell Au atom replaced by a Cd atom (see Figure 3 and supporting CIF files), which was also supported by computations: The experimental UV/vis/NIR spectrum was well reproduced by time-dependent density functional theory (TDDFT) calculations;[40] see Figure S8. It is known that, for $[Au_{25}]^-$, the lowest energy band at ~680 nm corresponds to an intraband (sp←sp) transition, and the featured band at ~450 nm arise from mixed intraband (sp←sp) and interband (sp←d) transitions, while the band centered at ~400 nm arises principally from an interband transition (sp←d).[17] The doping of Cd greatly tunes the electronic structure of $[Au_{25}]^-$ (Figures S9 and S10, and Tables S1 and S2). Different from the cases of $[Au_{25}]^-$, the ~658 nm absorption of $Au_{24}Cd(PET)_{18}$ can be assigned to the mixed intraband (sp←sp) and interband (sp←d) transitions (primary transitions

DOI: 10.1021/jacs.5b09627
J. Am. Chem. Soc. 2015, 137, 15350−15353

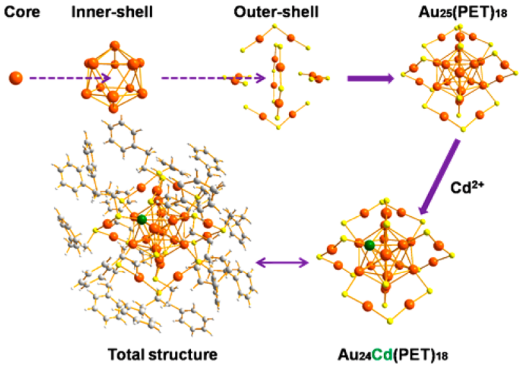

Figure 3. Structure anatomy of $Au_{25}(PET)_{18}$ and the crystal structure of $Au_{24}Cd(PET)_{18}$.

include HOMO → LUMO+4, HOMO−1 → LUMO+3, HOMO−4 → LUMO+1, HOMO−8 → LUMO), and the peaks at ∼553 and ∼474 nm also arise from both intraband (sp←sp) and interband (sp←d) transitions (for their respective primary transitions, see Figure S9). Compared with the cases of $[Au_{25}]^-$, the energy level spacings of $Au_{24}Cd$ are more uniform, and the LUMOs of $Au_{24}Cd$ are additionally contributed by the d atomic orbital of Au. Thus, the prominent change in the electronic structure of $[Au_{25}]^-$ upon Cd doping results in the obvious shift of the featured absorption peaks of $[Au_{25}]^-$.

The Cd doping mode in this work is consistent with some previous predictions,[31] but differs from the recently reported Hg doping, where one of the outer-shell Au atoms of Au_{25} was replaced by a Hg atom.[57] The UV/vis/NIR spectra indicate an obvious difference between the two dopings: for $Au_{24}Cd$, the maximum absorption in the long-wavelength range lies at ∼658 nm, while for $Au_{24}Hg$, it moves to ∼700 nm; see Figure S11. The fragmentation modes in MALDI-MS also exhibit a distinct difference between the two DTNs: the Cd is included in the closed fragments of the molecular ions (see Figure 2), while Hg is not (see Figure S12), which may explain why the heteroatoms occupy different sites for these two DTNs. Note that the Cd doping is also different from the previous Pt or Pd doping, where the central Au of Au_{25} is replaced by the invasive foreign atom.[25,37,38,64] The Cd doping in this work is distinctly different from a very recent one, too, where Cd was located at the core of the nanocluster.[27] We reproduced the single-crystal X-ray data at different temperatures (123 K or 258 K, see Supporting Information, CIF data), to exclude the influence of the X-ray measurement temperature. Possible reasons are the differences in synthesis and treatment before single-crystal X-ray data were collected in these two works. Of note, we did find that AGR is ion-precursor and ion-dose dependent[65] and that isomerism exists in nanoclusters[66] in previous works. More interestingly, the $Au_{24}Cd$ can be transformed to $Au_{24}Hg$[57] immediately (in 1 min) after the addition of 1 equiv of Hg^{2+}; see Figures 4 and S12. By contrast, the transformation from $Au_{24}Hg$[57] to $Au_{24}Cd$ is not successful under all the investigated conditions (including various temperatures and molar ratios; see Figure 4, inset). The fast transformation from $Au_{24}Cd$ to $Au_{24}Hg$ demonstrates that the reaction $Au_{24}Cd + Hg^{2+} \rightarrow Au_{24}Hg + Cd^{2+}$ is kinetically favorable, and computations revealed that replacement of the inner-shell Cd by Hg is also thermodynamically favorable (∼ −3.5 kcal/mol) at 25 °C, which somewhat explains the irreversibility of the transformation from $Au_{24}Cd(PET)_{18}$ to $Au_{24}Hg(PET)_{18}$. Another explanation for this irreversibility is that the replacement of Cd in $Au_{24}Cd$ by Hg can be regarded as a

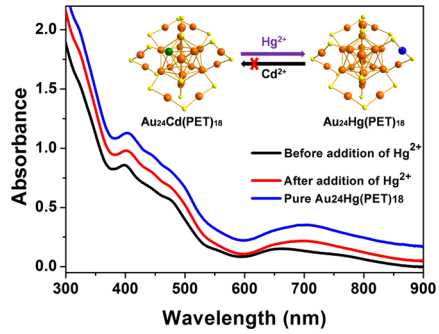

Figure 4. UV/vis/NIR absorption spectra of $Au_{24}Cd(PET)_{18}$ before (black) and after (red) addition of 1 equiv of Hg^{2+} and pure $Au_{24}Hg(PET)_{18}$ (blue) for comparison. Inset illustrates the irreversible transformation from $Au_{24}Cd(PET)_{18}$ to $Au_{24}Hg(PET)_{18}$.

spontaneous GR, while the replacement of Hg in $Au_{24}Hg$ by Cd is an AGR process, which is inhibited by the limited reduction ability of $Au_{24}Hg$ (or limited oxidation ability of Cd^{2+}). Of note, it is unexpected that replacement of the Cd atom of $Au_{24}Cd$ with Hg leads to Hg occupying the outer-shell, and a likely mechanism is that a thermodynamically favorable structure recombination (isomerization[66,67]) leads to the migration of dopant position from the icosahedron surface to outer-shell (surface segregation[67]) following the inner-shell Cd−Hg exchange. For the detailed mechanism, the solution system is rather complex and needs to be further investigated in the future.

In summary, we have demonstrated that $[Au_{25}]^-$ can react with some active metal ions (Zn^{2+}, Co^{2+}, Ni^{2+}, and Cd^{2+}) in an ion-dependent fashion: $[Au_{25}]^-$ can be oxidized to $[Au_{25}]^0$ by Co^{2+} and Ni^{2+}, to $[Au_{25}]^+$ by Zn^{2+}, and to $[Au_{25}]^0$ and $Au_{24}Cd(PET)_{18}$ by Cd^{2+}. Importantly, atomically mono-disperse $Au_{24}Cd(PET)_{18}$ is isolated in 56% yield, and its structure was revealed by single-crystal X-ray diffraction, which demonstrates that one of the inner-shell Au atoms in Au_{25} is replaced by a Cd atom, differing from the outer-shell Hg doping and the central Pd (or Pt) doping. Specifically, it is found that Hg and Cd exhibit different doping modes and effects, although they have similar electron structures. In addition, the $Au_{24}Cd(PET)_{18}$ can be irreversibly transformed to $Au_{24}Hg(PET)_{18}$. Further investigations are underway in our laboratory. These interesting results demonstrate the versatility of AGR, have important implications for structure (composition)−property correlations, and could stimulate more research on the subtle tuning of the compositions, structures, and properties of metal nanoclusters (nanoparticles) by precise doping in the future.

■ ASSOCIATED CONTENT

Supporting Information

The Supporting Information is available free of charge on the ACS Publications website at DOI: 10.1021/jacs.5b09627.

Experimental details; MALDI-TOF-MS, UV/vis/NIR, TGA data; TDDFT simulation; Kohn−Sham orbital energy level diagram; and structural data (PDF)
X-ray file for $Au_{24}Cd(PET)_{18}$ at 258 K (CIF)
X-ray file for $Au_{24}Cd(PET)_{18}$ at 123 K (CIF)

■ AUTHOR INFORMATION

Corresponding Authors

*zkwu@issp.ac.cn
*jlyang@ustc.edu.cn
*lhweng@fudan.edu.cn

DOI: 10.1021/jacs.5b09627
J. Am. Chem. Soc. 2015, 137, 15350−15353

Author Contributions

[§]C.Y., Y.L., J.Y. contributed equally.

Notes

The authors declare no competing financial interest.

■ ACKNOWLEDGMENTS

We acknowledge financial support from National Basic Research Program of China (Grant No. 2013CB934302), Natural Science Foundation of China (Nos. 21222301, 21171170, 21401064), Ministry of Human Resources and Social Security of China, Innovative Program of Development Foundation of Hefei Center for Physical Science and Technology (2014FXCX002), Hefei Science Center, CAS (user of potential: 2015HSC-UP003), CAS/SAFEA International Partnership Program for Creative Research Teams, and the "Hundred Talents Program" of Chinese Academy of Sciences. The calculations in this paper have been done on the supercomputing system in the Supercomputing Center of University of Science and Technology of China.

■ REFERENCES

(1) Linic, S.; Christopher, P.; Xin, H.; Marimuthu, A. *Acc. Chem. Res.* **2013**, *46*, 1890.
(2) Saha, K.; Agasti, S.; Kim, C.; Li, X.; Rotello, V. M. *Chem. Rev.* **2012**, *112*, 2739.
(3) Jin, R.; Cao, Y.; Mirkin, C. A.; Kelly, K. L.; Schatz, G. C.; Zheng, J. G. *Science* **2001**, *294*, 1901.
(4) Gao, F.; Goodman, D. W. *Chem. Soc. Rev.* **2012**, *41*, 8009.
(5) Link, S.; Wang, Z. L.; El-Sayed, M. A. *J. Phys. Chem. B* **1999**, *103*, 3529.
(6) Chen, Y.-H.; Yeh, C.-S. *Chem. Commun.* **2001**, 371.
(7) Shibata, T.; Bunker, B.; Zhang, Z.; Meisel, D.; Vardeman, C.; Gezelter, J. *J. Am. Chem. Soc.* **2002**, *124*, 11989.
(8) Ferrando, R.; Jellinek, J.; Johnston, R. *Chem. Rev.* **2008**, *108*, 845.
(9) Liu, X.; Wang, D.; Li, Y. *Nano Today* **2012**, *7*, 448.
(10) Le Guevel, X.; Trouillet, V.; Spies, C.; Li, K.; Laaksonen, T.; Auerbach, D.; Jung, G.; Schneider, M. *Nanoscale* **2012**, *4*, 7624.
(11) Dou, X.; Yuan, X.; Yu, Y.; Luo, Z.; Yao, Q.; Leong, D.; Xie, J. *Nanoscale* **2014**, *6*, 157.
(12) Price, R. C.; Whetten, R. L. *J. Am. Chem. Soc.* **2005**, *127*, 13750.
(13) Negishi, Y.; Chaki, N. K.; Shichibu, Y.; Whetten, R. L.; Tsukuda, T. *J. Am. Chem. Soc.* **2007**, *129*, 11322.
(14) Luo, Z.; Nachammai, V.; Zhang, B.; Yan, N.; Leong, D. T.; Jiang, D.-e.; Xie, J. *J. Am. Chem. Soc.* **2014**, *136*, 10577.
(15) Jadzinsky, P.; Calero, G.; Ackerson, C.; Bushnell, D.; Kornberg, R. *Science* **2007**, *318*, 430.
(16) Heaven, M. W.; Dass, A.; White, P. S.; Holt, K. M.; Murray, R. W. *J. Am. Chem. Soc.* **2008**, *130*, 3754.
(17) Zhu, M.; Aikens, C. M.; Hollander, F. J.; Schatz, G. C.; Jin, R. *J. Am. Chem. Soc.* **2008**, *130*, 5883.
(18) Lopez-Acevedo, O.; Tsunoyama, H.; Tsukuda, T.; Häkkinen, H.; Aikens, C. M. *J. Am. Chem. Soc.* **2010**, *132*, 8210.
(19) Qian, H.; Zhu, M.; Wu, Z.; Jin, R. *Acc. Chem. Res.* **2012**, *45*, 1470.
(20) Jin, R.; Nobusada, K. *Nano Res.* **2014**, *7*, 285.
(21) Joshi, C.; Bootharaju, M.; Alhilaly, M.; Bakr, O. *J. Am. Chem. Soc.* **2015**, *137*, 11578.
(22) Yang, H.; Wang, Y.; Huang, H.; Gell, L.; Lehtovaara, L.; Malola, S.; Häkkinen, H.; Zheng, N. *Nat. Commun.* **2013**, *4*, 2422.
(23) Udayabhaskararao, T.; Sun, Y.; Goswami, N.; Pal, S.; Balasubramanian, K.; Pradeep, T. *Angew. Chem., Int. Ed.* **2012**, *51*, 2155.
(24) Barrabes, N.; Zhang, B.; Burgi, T. *J. Am. Chem. Soc.* **2014**, *136*, 14361.
(25) Qian, H.; Jiang, D.-e.; Li, G.; Gayathri, C.; Das, A.; Gil, R.; Jin, R. *J. Am. Chem. Soc.* **2012**, *134*, 16159.
(26) Christensen, S.; MacDonald, M.; Chatt, A.; Zhang, P.; Qian, H.; Jin, R. *J. Phys. Chem. C* **2012**, *116*, 26932.
(27) Wang, S.; Song, Y.; Jin, S.; Liu, X.; Zhang, J.; Pei, Y.; Meng, X.; Chen, M.; Li, P.; Zhu, M. *J. Am. Chem. Soc.* **2015**, *137*, 4018.
(28) Guidez, E.; Makinen, V.; Häkkinen, H.; Aikens, C. *J. Phys. Chem. C* **2012**, *116*, 20617.
(29) Jiang, D.-e.; Dai, S. *Inorg. Chem.* **2009**, *48*, 2720.
(30) Malola, S.; Häkkinen, H. *J. Phys. Chem. Lett.* **2011**, *2*, 2316.
(31) Walter, M.; Moseler, M. *J. Phys. Chem. C* **2009**, *113*, 15834.
(32) Kwak, K.; Tang, Q.; Kim, M.; Jiang, D.-e.; Lee, D. *J. Am. Chem. Soc.* **2015**, *137*, 10833.
(33) Xiao, N.; Xu, Q.; Tsubota, S.; Sun, J.; Chen, J. *Organometallics* **2002**, *21*, 2764.
(34) Bouherour, S.; Braunstein, P.; Rose, J.; Toupet, L. *Organometallics* **1999**, *18*, 4908.
(35) McGrath, T. D.; Du, S.; Hodson, B. E.; Stone, F. G. A. *Organometallics* **2006**, *25*, 4452.
(36) Mathur, P.; Mukhopadhyay, S.; Ahmed, M. O.; Lahiri, G. K.; Chakraborty, S.; Walawalkar, M. G. *Organometallics* **2000**, *19*, 5787.
(37) Miller, S.; Fields-Zinna, C.; Murray, R.; Moran, A. *J. Phys. Chem. Lett.* **2010**, *1*, 1383.
(38) Negishi, Y.; Kurashige, W.; Niihori, Y.; Iwasa, T.; Nobusada, K. *Phys. Chem. Chem. Phys.* **2010**, *12*, 6219.
(39) Kauffman, D.; Alfonso, D.; Matranga, C.; Qian, H.; Jin, R. *J. Phys. Chem. C* **2013**, *117*, 7914.
(40) Kumara, C.; Aikens, C.; Dass, A. *J. Phys. Chem. Lett.* **2014**, *5*, 461.
(41) Kumara, C.; Dass, A. *Nanoscale* **2011**, *3*, 3064.
(42) Kumara, C.; Gagnon, K.; Dass, A. *J. Phys. Chem. Lett.* **2015**, *6*, 1223.
(43) Dharmaratne, A.; Dass, A. *Chem. Commun.* **2014**, *50*, 1722.
(44) Yan, J.; Su, H.; Yang, H.; Malola, S.; Lin, S.; Häkkinen, H.; Zheng, N. *J. Am. Chem. Soc.* **2015**, *137*, 11880.
(45) Zhang, L.; Wang, Y.; Tong, L.; Xia, Y. *Nano Lett.* **2014**, *14*, 4189.
(46) Xia, X.; Wang, Y.; Ruditskiy, A.; Xia, Y. *Adv. Mater.* **2013**, *25*, 6313.
(47) Wan, D.; Xia, X.; Wang, Y.; Xia, Y. *Small* **2013**, *9*, 3111.
(48) da Silva, A.; de Souza, M.; Rodrigues, T.; Alves, R.; Temperini, M.; Camargo, P. *Chem. - Eur. J.* **2014**, *20*, 15040.
(49) Coleman, E.; Co, A. *J. Catal.* **2014**, *316*, 191.
(50) Liu, M.; Zheng, Y.; Xie, S.; Li, N.; Lu, N.; Wang, J.; Kim, M.; Guo, L.; Xia, Y. *Phys. Chem. Chem. Phys.* **2013**, *15*, 11822.
(51) Sarkar, A.; Manthiram, A. *J. Phys. Chem. C* **2010**, *114*, 4725.
(52) Huang, T.-K.; Cheng, T.-H.; Yen, M.-Y.; Hsiao, W.-H.; Wang, L.-S.; Chen, F.-R.; Kai, J.-J.; Lee, C.-Y.; Chiu, H.-T. *Langmuir* **2007**, *23*, 5722.
(53) Kim, K.; Kim, S.; Choi, S.; Kim, J.; Lee, I. *ACS Nano* **2012**, *6*, 5122.
(54) Skrabalak, S.; Chen, J.; Sun, Y.; Lu, X.; Au, L.; Cobley, C.; Xia, Y. *Acc. Chem. Res.* **2008**, *41*, 1587.
(55) Wu, Z. *Angew. Chem., Int. Ed.* **2012**, *51*, 2934.
(56) Yao, C.; Chen, J.; Li, M.-B.; Liu, L.; Yang, J.; Wu, Z. *Nano Lett.* **2015**, *15*, 1281.
(57) Liao, L.; Zhou, S.; Dai, Y.; Liu, L.; Yao, C.; Fu, C.; Yang, J.; Wu, Z. *J. Am. Chem. Soc.* **2015**, *137*, 9511.
(58) Wu, Z.; Suhan, J.; Jin, R. *J. Mater. Chem.* **2009**, *19*, 622.
(59) Wu, Z.; Jin, R. *Nano Lett.* **2010**, *10*, 2568.
(60) Antonello, S.; Perera, N.; Ruzzi, M.; Gascon, J.; Maran, F. *J. Am. Chem. Soc.* **2013**, *135*, 15585.
(61) Venzo, A.; Antonello, S.; Gascon, J.; Guryanov, I.; Leapman, R.; Perera, N.; Sousa, A.; Zamuner, M.; Zanella, A.; Maran, F. *Anal. Chem.* **2011**, *83*, 6355.
(62) Liu, Z.; Zhu, M.; Meng, X.; Xu, G.; Jin, R. *J. Phys. Chem. Lett.* **2011**, *2*, 2104.
(63) Zhu, M.; Eckenhoff, W.; Pintauer, T.; Jin, R. *J. Phys. Chem. C* **2008**, *112*, 14221.
(64) Kacprzak, K. A.; Lehtovaara, L.; Akola, J.; Lopez-Acevedo, O.; Häkkinen, H. *Phys. Chem. Chem. Phys.* **2009**, *11*, 7123.
(65) Tian, S.; Yao, C.; Liao, L.; Xia, N.; Wu, Z. *Chem. Commun.* **2015**, *51*, 11773.
(66) Tian, S.; Li, Y.-Z.; Li, M.-B.; Yuan, J.; Yang, J.; Wu, Z.; Jin, R. *Nat. Commun.* **2015**, *6*, 8667.
(67) Liao, H.; Fisher, A.; Xu, Z. J. *Small* **2015**, *11*, 3221.

DOI: 10.1021/jacs.5b09627
J. Am. Chem. Soc. 2015, 137, 15350−15353